



Enright, J. M., Toomey, M. B., Sato, S., Temple, S., Allen, J. R., Fujiwara, R., ... Corbo, J. (2015). Cyp27c1 red-shifts the spectral sensitivity of photoreceptors by converting Vitamin A<sub>1</sub> into A<sub>2</sub>. *Current Biology*, 25(23), 3048-3057. <https://doi.org/10.1016/j.cub.2015.10.018>

Peer reviewed version

License (if available):  
Unspecified

Link to published version (if available):  
[10.1016/j.cub.2015.10.018](https://doi.org/10.1016/j.cub.2015.10.018)

[Link to publication record in Explore Bristol Research](#)  
PDF-document

Copyright © 2015 Elsevier Inc

## University of Bristol - Explore Bristol Research

### General rights

This document is made available in accordance with publisher policies. Please cite only the published version using the reference above. Full terms of use are available:  
<http://www.bristol.ac.uk/pure/about/ebr-terms>

# Cyp27c1 Red-Shifts the Spectral Sensitivity of Photoreceptors by Converting Vitamin A1 into A2

Jennifer M. Enright,<sup>1</sup> Matthew B. Toomey,<sup>1</sup> Shin-ya Sato,<sup>2</sup> Shelby E. Temple,<sup>3</sup> James R. Allen,<sup>4</sup> Rina Fujiwara,<sup>5</sup> Valerie M. Kramlinger,<sup>5</sup> Leslie D. Nagy,<sup>5</sup> Kevin M. Johnson,<sup>5</sup> Yi Xiao,<sup>5</sup> Martin J. How,<sup>3</sup> Stephen L. Johnson,<sup>4</sup> Nicholas W. Roberts,<sup>3</sup> Vladimir J. Kefalov,<sup>2</sup> F. Peter Guengerich,<sup>5</sup> and Joseph C. Corbo<sup>1,\*</sup>

<sup>1</sup>Department of Pathology and Immunology, Washington University School of Medicine, St. Louis, MO 63110, USA

<sup>2</sup>Department of Ophthalmology and Visual Sciences, Washington University School of Medicine, St. Louis, MO 63110, USA

<sup>3</sup>School of Biological Sciences, University of Bristol, Bristol BS8 1TQ, UK

<sup>4</sup>Department of Genetics, Washington University School of Medicine, St. Louis, MO 63110, USA

<sup>5</sup>Department of Biochemistry, Vanderbilt University School of Medicine, Nashville, TN 37232, USA

## SUMMARY

Some vertebrate species have evolved means of extending their visual sensitivity beyond the range of human vision. One mechanism of enhancing sensitivity to long-wavelength light is to replace the 11-cis retinal chromophore in photopigments with 11-cis 3,4-didehydroretinal. Despite over a century of research on this topic, the enzymatic basis of this perceptual switch remains unknown. Here, we show that a cytochrome P450 family member, Cyp27c1, mediates this switch by converting vitamin A1 (the precursor of 11-cis retinal) into vitamin A2 (the precursor of 11-cis 3,4-didehydroretinal). Knockout of *cyp27c1* in zebrafish abrogates production of vitamin A2, eliminating the animal's ability to red-shift its photoreceptor spectral sensitivity and reducing its ability to see and respond to near-infrared light. Thus, the expression of a single enzyme mediates dynamic spectral tuning of the entire visual system by controlling the balance of vitamin A1 and A2 in the eye.

## INTRODUCTION

The visual pigments of vertebrate rod and cone photoreceptors consist of a G-protein-coupled receptor, the opsin, and a covalently bound chromophore, most commonly 11-cis retinal [1]. Vision begins when a photon of light induces a cis to trans isomerization of the chromophore, thereby altering the conformation of the opsin and, in turn, activating the phototransduction cascade [1, 2]. The spectral sensitivity of a visual pigment is determined by the structure of the chromophore and the electrostatic and steric interactions between the chromophore and the amino acid side chains within the binding cleft of the opsin [3, 4].

Typical rod photopigments have a maximum absorbance ( $I_{max}$ ) of around 500 nm [5]. However, it was first noted in the 19th century that certain freshwater fishes have rod photopigments whose  $I_{max}$  values are red-shifted by 20–30 nm relative to those of marine fishes and terrestrial vertebrates [6, 7]. The spectral sensitivity of cone photoreceptors is also red-shifted in freshwater species, in some cases by as much as 60 nm [8]. This red-shift is caused by replacement of the chromophore, 11-cis retinal, with 11-cis 3,4-didehydroretinal, which contains an additional conjugated double bond within its b-ionone ring (Figure 1A) [14]. Rod photopigments containing 11-cis retinal are referred to as “rhodopsins” on account of the rose-colored appearance of the unbleached pigment, whereas those containing 11-cis 3,4-didehydroretinal are called “porphyropsins” on account of their purple color [7, 12, 14]. Therefore, the change in chromophore from 11-cis retinal to 11-cis 3,4-didehydroretinal is referred to as the “rhodopsin-to-porphyropsin” switch.

This switch is believed to result in a better match between the sensitivity of the visual system and the spectral distribution of light in fresh water, which is often red-shifted relative to

marine and terrestrial environments [12, 14, 15]. 3,4-didehydroretinoids have been identified in the

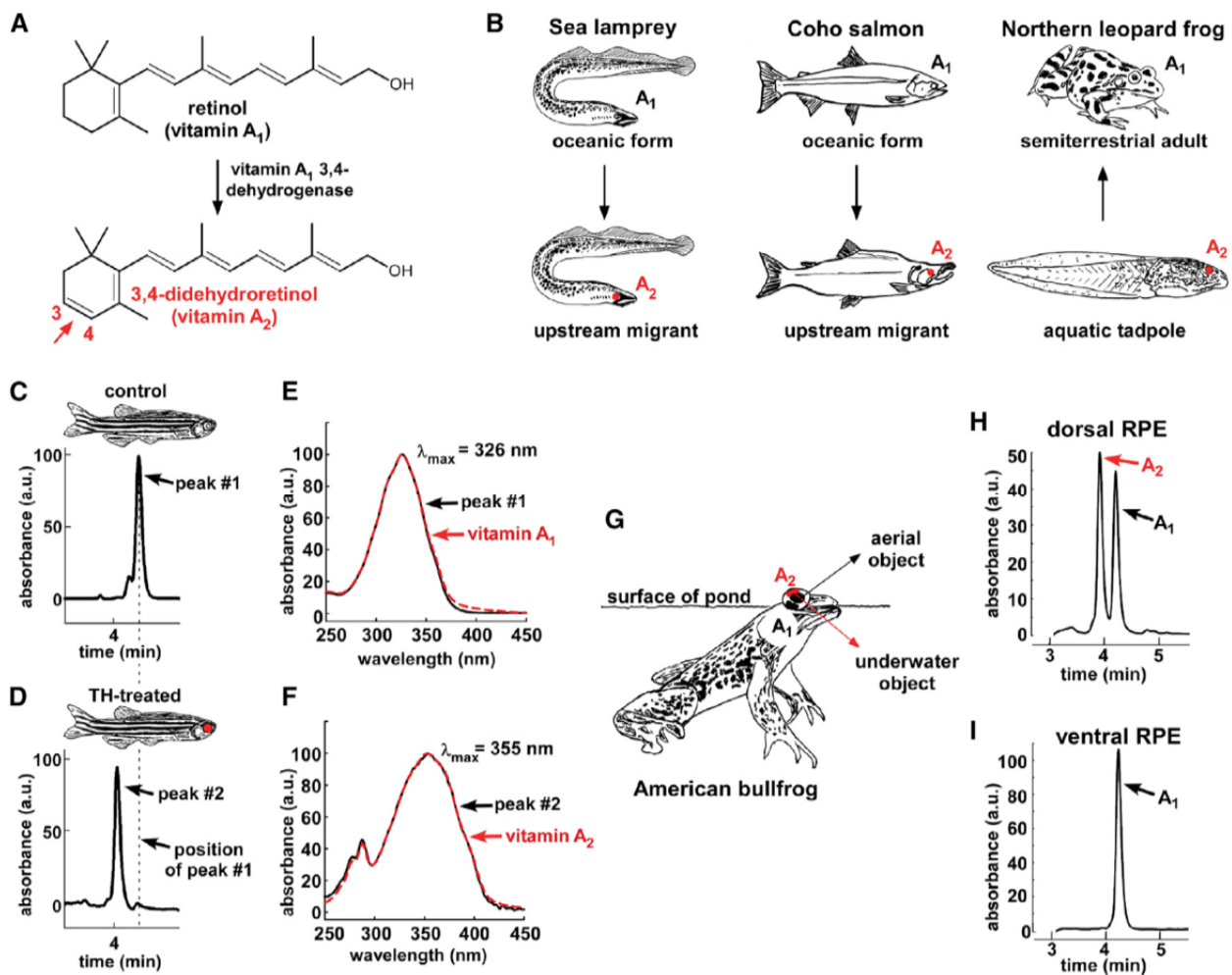


Figure 1. Modeling the Rhodopsin-Porphyrpsin Switch

(A) The conversion of retinol (vitamin A<sub>1</sub>) to 3,4-didehydroretinol (vitamin A<sub>2</sub>) underlies the rhodopsin-to-porphyrpsin switch and is driven by a previously unidentified dehydrogenase that catalyzes the addition of a double bond to the b-ionone ring.

(B) This vitamin A<sub>1</sub> to A<sub>2</sub> switch is widely used by a variety of vertebrates and can be deployed at key stages of the life cycle: e.g., during upstream migration in sea lamprey (*Petromyzon marinus*) and Coho salmon (*Oncorhynchus kisutch*) and upon metamorphosis in amphibians such as the northern leopard frog (*Lithobates pipiens*) [9–11].

(C and D) To model this switch, zebrafish were treated with thyroid hormone (300 mg/l L-thyroxine [T4]) for 3 weeks. Retinoids were then isolated from pooled RPE and retina of three individuals, reduced using sodium borohydride, and analyzed by HPLC. Retinoids from TH-treated fish have a shorter retention time than those from vehicle-treated fish.

(E) The absorbance spectrum of the predominant retinoid from control fish closely matches the absorbance spectrum of a vitamin A<sub>1</sub> standard, with a  $\lambda_{max}$  of 326 nm.

(F) The predominant retinoid from TH-treated fish has an absorbance spectrum that matches that of the vitamin A<sub>2</sub> standard, with a  $\lambda_{max}$  of 355 nm.

(G) The American bullfrog (*Lithobates catesbeianus*) often sits at the water's surface and possesses exclusively A<sub>1</sub>-based visual pigments in the ventral retina and a mixture of A<sub>1</sub>- and A<sub>2</sub>-based visual pigments in the dorsal retina, possibly facilitating downward vision into the murky, red-shifted water [12, 13].

(H and I) The dorsal third of the RPE from two American bullfrogs was dissected, pooled, and analyzed by HPLC and found to contain a mixture of vitamin A<sub>1</sub> and vitamin A<sub>2</sub>. Only vitamin A<sub>1</sub> was identified in the ventral third of the RPE. All absorbance values are normalized and represented as arbitrary units (a.u.).

eyes of the vast majority of freshwater fish and amphibian species that have been examined [15, 16]. This observation suggests that thousands of vertebrate species may use chromophore switching to tune

the spectral sensitivity of their visual systems. In addition, in many species of lampreys, fish, and amphibians, the visual system is dynamically tuned by altering the balance of 11-cis retinal and 11-cis 3,4-didehydroretinal in the retina when the animal moves between different light environments [9–11, 15, 17]. For example, the ratio of 11-cis 3,4-didehydroretinal to 11-cis retinal increases when

species such as salmon or sea lamprey migrate from the open ocean into inland freshwater environments (Figure 1B) [9, 11]. Conversely, many amphibians use 11-cis 3,4-didehydroretinal during the freshwater tadpole stage but then switch to 11-cis retinal upon metamorphosis into a terrestrial adult (Figure 1B) [10, 15, 17]. Although several environmental factors, including changes in temperature or season, may affect the balance of the two chromophores [15, 18], there is clearly a strong correlation between the red-shifted light environment of freshwater habitats and the use of the red-shifted chromophore, 11-cis 3,4-didehydroretinal [9, 11, 12, 15].

Despite many decades of research on the rhodopsin-porphyrin system, the enzyme that mediates this switch has been unknown. In this study, we employed transcriptome profiling of distantly related fish and amphibian models to identify the enzyme responsible for converting retinol into 3,4-didehydroretinol (henceforth referred to as vitamin A1 and vitamin A2, respectively). We confirmed that this enzyme is required for the red-shift in photoreceptor sensitivity that occurs upon chromophore exchange *in vivo* and demonstrated that this change in sensitivity enhances the fish's ability to see and respond to near-infrared light.

## RESULTS

### Animal Models of the Vitamin A1/A2 Switch

To identify the enzyme responsible for converting vitamin A1 into vitamin A2, we used zebrafish (*Danio rerio*) and American bullfrog (*Lithobates catesbeianus*) models. Zebrafish photoreceptors predominantly contain vitamin A1-based visual pigments under normal laboratory conditions, but treatment with thyroid hormone (TH) induces a conversion to vitamin A2-based pigments [19]. To corroborate this result, we treated zebrafish with TH and then analyzed the retinoid content of retinas and retinal pigment epithelium (RPE) by high-performance liquid chromatography (HPLC). We found a nearly complete conversion of vitamin A1 into vitamin A2 in the TH-treated animals (Figures 1C–1F).

Next, we analyzed a specialized pattern of regional chromophore localization within the American bullfrog retina. Most amphibians employ A2-based visual pigments during the aquatic phase of their life cycle, switching to predominantly A1-based pigments after metamorphosis [10, 15, 17]. However, American bullfrogs retain A2-based pigments in the dorsal third of their retinas and RPE, even as adults (Figure 1G) [12]. Because adult bullfrogs spend a considerable amount of time with their eyes just above the water's surface [13], the presence of vitamin A2-based pigments in the dorsal retina has been speculated to facilitate downward vision into the murky, red-shifted aquatic environment [12]. We dissected dorsal and ventral RPE from adult American bullfrogs, extracted retinoids, and analyzed them by HPLC. Whereas the ventral RPE contained exclusively vitamin A1 and its derivatives, the dorsal RPE contained a mixture of vitamin A1 and A2 (Figures 1H and 1I). Thus, both TH-treated zebrafish and American bullfrog represent suitable model systems for analyzing the mechanistic basis of the rhodopsin-porphyrin switch.

### Identifying a Candidate Enzyme

The RPE plays a critical role in regenerating 11-cis retinal and is the locus of vitamin A1 to A2 conversion in some species [12, 20, 21]. Therefore, to identify candidate genes that might encode the vitamin A1 3,4-dehydrogenase, we profiled zebrafish and bullfrog RPE by RNA-seq. We compared the transcriptomes of RPE from TH-treated zebrafish with that of vehicle-treated controls, identifying a total of 35 TH-upregulated genes (Figure 2A; Table S1). We also compared dorsal and ventral RPE from adult bullfrogs, identifying a total of 40 dorsally enriched genes (Figure 2B; Table

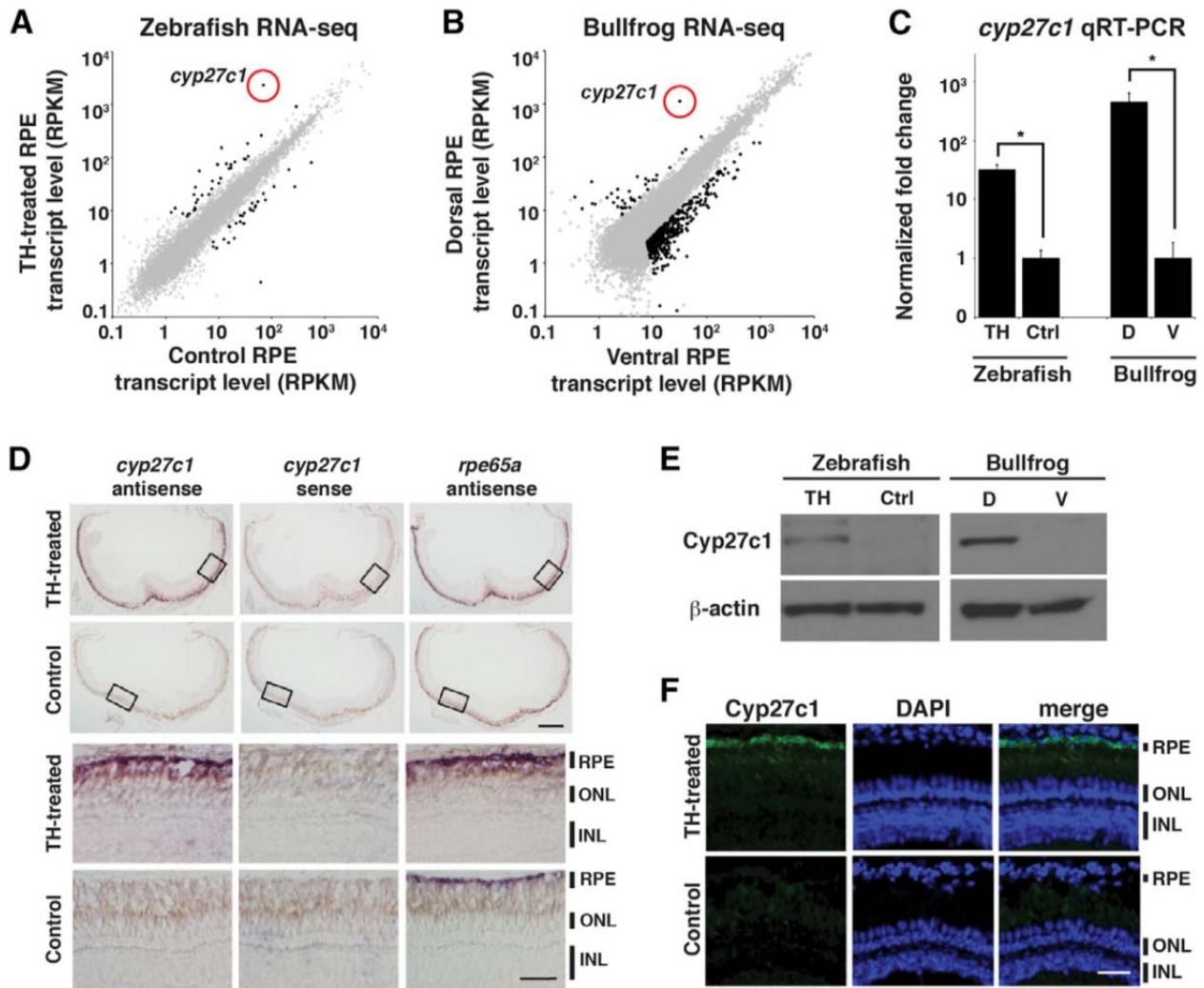


**Figure 2. Cyp27c1 Expression Is Correlated with the Presence of Vitamin A<sub>2</sub> in Zebrafish and Bullfrog RPE**  
 (A) Zebrafish were treated with TH or a vehicle control for 3 weeks, after which RPE was isolated and used to construct a cDNA library for transcriptome profiling by RNA-seq. Expression levels (in RPKM [reads per kilobase of transcript per million mapped reads]) of individual transcripts from TH-treated RPE (y axis) and vehicle-treated RPE (x axis) are shown as dots, with significantly differentially expressed genes in black (quantile-adjusted conditional maximum likelihood [qCML] test; FDR < 0.05; n = 3).  
 (B) Dorsal and ventral thirds of bullfrog RPE were isolated and used to construct a cDNA library for transcriptome profiling by RNA-seq. Expression levels of individual transcripts from dorsal RPE (y axis) and ventral RPE (x axis) are shown as dots, with significantly differentially expressed genes in black (qCML test; FDR < 0.05; n = 3).  
 (C) Enrichment of the *cyp27c1* transcript in cDNA samples used for RNA-seq was confirmed by quantitative real-time PCR (qRT-PCR). Expression was normalized to ribosomal protein *rpl13a* for zebrafish and *rpl7a* for bullfrog (two-sided Student's t test; n = 2–3; \*p < 0.005; error bars = SEM).  
 (D) In situ hybridization of albino zebrafish treated with TH or vehicle control for 3 weeks. Top panels show cross-sections of the whole eye. Bottom panels show high-magnification images of the boxed regions from the top panels. The antisense probe for *cyp27c1* localized exclusively to the RPE in TH-treated fish. No signal was observed with the *cyp27c1* sense probe, but strong signal was observed in the RPE of TH-treated and control fish with an antisense probe against *rpe65a*, a gene that is expressed at high levels in RPE. The scale bars represent 200 mm low power and 50 mm high power.  
 (E) Western blot with a rabbit polyclonal anti-Cyp27c1 antibody confirmed enrichment of Cyp27c1 protein in TH-treated zebrafish and dorsal bullfrog RPE. *b-actin* was used as a loading control.  
 (F) Immunohistochemistry of albino TH- and vehicle-treated zebrafish indicates induction of Cyp27c1 expression in the RPE of TH-treated fish (green), with DAPI used to counter-stain nuclei (blue). The scale bar represents 50 mm.  
 See also [Figure S1](#) and [Tables S1](#) and [S2](#).

S2). In both analyses, one candidate gene stood out as being among the most highly upregulated and enriched, the cytochrome P450 family member, *cyp27c1* (Figures 2A and 2B). Members of the P450 family are involved in the metabolism of a variety of xenobiotics and endogenous small molecules including retinoids, although a functional role for *cyp27c1* has not previously been reported [22–25]. Thus, Cyp27c1 is an excellent candidate for the vitamin A<sub>1</sub> 3,4-dehydrogenase.

To determine whether the presence of *cyp27c1* correlates with the distribution of vitamin A2 and its derivatives, we analyzed *cyp27c1* expression in zebrafish and bullfrog eyes. We first confirmed that the *cyp27c1* transcript is significantly increased in TH-treated zebrafish RPE and dorsal bullfrog RPE by quantitative real-time PCR (Figure 2C). We then determined the cellular expression pattern of *cyp27c1*, by performing in situ hybridization on eyes from TH-treated albino zebrafish and vehicle controls [26]. The albino strain was used to improve visualization of staining in the RPE, and we confirmed that it undergoes a TH-dependent switch to vitamin A2 similar to wild-type strains (data not shown). The *cyp27c1* antisense probe localized exclusively to the RPE after TH treatment, with no signal observed in the vehicle-treated control eyes (Figure 2D). In contrast, the RPE-specific transcript, *rpe65a*, was detected in both TH- and vehicle-treated eyes, confirming the presence of RPE in the sections (Figure 2D). Taken together, these results indicate a specific upregulation of *cyp27c1* in the RPE of TH-treated fish and are consistent with a previous report suggesting that the RPE is the primary locus of vitamin A2 production in some species [12].

To assay the expression levels of Cyp27c1 protein in zebrafish and bullfrog RPE, we raised a polyclonal anti-Cyp27c1 antibody in rabbit and confirmed its activity against Cyp27c1 produced in HEK293 cell culture (Figure S1). We then used this antibody in a western blot to confirm the induction of Cyp27c1 protein in TH-treated zebrafish RPE and its enrichment in dorsal bullfrog RPE (Figure 2E). In addition, using immunohistochemistry, we determined that Cyp27c1 protein is localized specifically to the RPE of TH-treated, but not control, albino zebrafish, in a pattern consistent with the *cyp27c1* transcript (Figures 2D and 2F). Overall, the distribution of both the *cyp27c1* transcript and protein correspond precisely to the pattern of vitamin A2 production in zebrafish and bullfrog.

### **Cyp27c1 Generates Vitamin A2 In Vitro**

To test whether Cyp27c1 is sufficient to produce vitamin A2, we expressed Cyp27c1 in HEK293 cells, which were then incubated with vitamin A1 for 24 hr and subjected to HPLC to assess retinoid content. Cells transfected with an empty vector contained only the vitamin A1 substrate, whereas cells transfected with the Cyp27c1 expression construct contained vitamin A2 in addition to vitamin A1 (Figure 3A). To further characterize enzyme kinetics, we expressed and purified Cyp27c1 and determined its catalytic efficiency with three different retinoid substrates: all-trans retinol, retinal, and retinoic acid. Cyp27c1 can act on all three substrates but most efficiently catalyzes the conversion of retinol (vitamin A1) to 3,4-didehydroretinol (vitamin A2; Figures 3B and S2). Furthermore, the catalytic efficiency of Cyp27c1 with vitamin A1 ( $k_{cat}/K_m = 1.4 \pm 0.5 \times 10^3 \text{ M}^{-1} \text{ min}^{-1}$ ) is among the higher values reported for animal cytochrome P450 family members [27–30]. These results confirm that Cyp27c1 has the requisite biochemical activity to mediate the rhodopsin-porphyrin switch.

### **Cyp27c1 Drives Vitamin A2 Production In Vivo**

If Cyp27c1 mediates the rhodopsin-porphyrin switch, zebrafish lacking this enzyme should not produce vitamin A2 in response to TH treatment. To test this hypothesis, we generated several mutant alleles of *cyp27c1* by using transcription activator-like effector nucleases (TALENs) to introduce small insertions/deletions within the first and fourth exons [31]. We obtained multiple alleles carrying frameshift mutations predicted to result in premature stop codons (Figures 4A and S3). Two independent lines were crossed to produce transheterozygous mutant fish (*cyp27c1D1/D2*), which survived to adulthood without overt developmental abnormalities. Upon

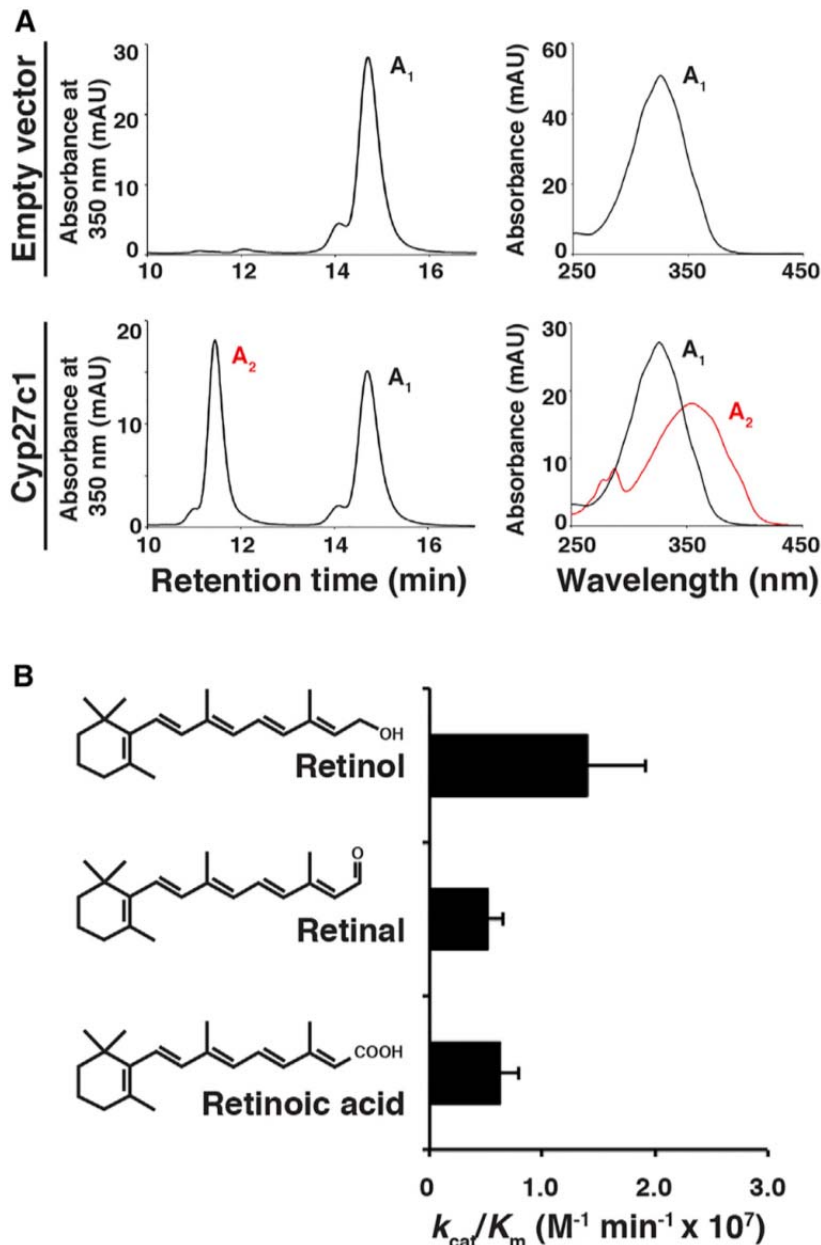


Figure 3. Cyp27c1 Is Sufficient to Convert Vitamin A<sub>1</sub> into Vitamin A<sub>2</sub> (A) HEK293 cells were transfected with a *cyp27c1* expression construct or an empty vector and incubated with vitamin A<sub>1</sub> for 24 hr, after which cells and media were harvested for HPLC. Cells transfected with empty vector did not produce vitamin A<sub>2</sub>, but cells transfected with *cyp27c1* converted a substantial fraction of the vitamin A<sub>1</sub> to vitamin A<sub>2</sub>. (B) A cell-free assay system was used to assess the catalytic efficiency of Cyp27c1 for all-trans retinol, retinal, and retinoic acid. Purified Cyp27c1 was incubated with bovine adrenodoxin (Adx), NADPH-adrenodoxin reductase (ADR), and substrate (with concentrations ranging from 0.1 to 10 mM). The reaction was then initiated using an NADPH-generating system, run for 60 s, and quenched. HPLC was used to quantify the products in order to calculate  $k_{cat}$  and  $K_m$ . A high catalytic efficiency ( $k_{cat}/K_m$ ) was observed for all three substrates. Error bars represent SEM. See also Figure S2.

treatment with TH, the mutant fish failed to produce Cyp27c1 protein, in contrast to their wild-type siblings (Figure 4B). We then used HPLC to assess retinoid content in the eyes of TH-treated *cyp27c1D1/D2* mutants and their wild-type siblings. Whereas a conversion to vitamin A<sub>2</sub> was observed in TH-treated wild-type fish, TH-treated *cyp27c1D1/D2* mutants failed to produce any vitamin A<sub>2</sub> (Figure 4C), indicating that Cyp27c1 is necessary for vitamin A<sub>2</sub> production in vivo. We also observed loss of vitamin A<sub>2</sub> production in fish carrying two additional heteroallelic combinations, *cyp27c1D1/D3* and *cyp27c1D4/D5* (Figure S3), indicating that this effect is attributable to the loss of Cyp27c1 rather than off-target mutations caused by the TALENs.

As TH-treated *cyp27c1D1/D2* fish fail to produce vitamin A<sub>2</sub> (the precursor of 11-cis 3,4-didehydroretinal), their photoreceptors should also fail to undergo a red-shift in sensitivity. To test this hypothesis, we used single-cell suction electrode recording to measure the sensitivity of individual red cones from

*cyp27c1D1/D2* mutants and wild-type siblings, treated with either TH or vehicle control. We measured red cones because they undergo the largest red-shift upon switching to 11-cis 3,4-didehydroretinal [19]. The flash sensitivity of individual red cones was determined from the amplitudes of their electrical responses to a series of dim flashes of 560-, 600-, 660-, and 700-nm light and fitted with a model that incorporates contributions from both vitamin A<sub>1</sub>- and A<sub>2</sub>-based



pigments [8]. No significant difference was observed between the sensitivities of vehicle-treated *cyp27c1D1/D2* and wild-type red cones at any of the wavelengths tested, and both wild-type and mutant red cones had maximal sensitivity ( $I_{max}$ ) at 561 nm, in close agreement with a previous estimate of  $I_{max} = 565$  nm, determined by MSP (Figures 4D and 4E) [19]. In addition, knockout of *cyp27c1* did not affect the dark current or the kinetics of the flash responses of the red cones, indicating that phototransduction remained intact (Figure 4E). In contrast, TH treatment induced a 57-nm redshift in the  $I_{max}$  of wild-type fish to 618 nm, whereas the  $I_{max}$  of TH-treated *cyp27c1D1/D2* mutant fish was unchanged (Figures 4D and 4E). Thus, knockout of *cyp27c1* completely eliminates the red-shift in red cone spectral sensitivity induced by TH treatment.

### **Behavioral Impact of Vitamin A2**

It has long been speculated that the switch from vitamin A1- to vitamin A2-based photopigments could be an adaptive response to changes in the animal's light environment, permitting the animal to adjust its spectral sensitivity to more closely match the spectral quality of its surroundings [9, 11, 12, 15]. The *cyp27c1* mutant zebrafish present an opportunity to test the relationship between vitamin A2 and behavioral responsiveness to longwavelength light. We therefore developed an assay to measure changes in swimming behavior in response to light of various wavelengths (Figures 5A–5C). When exposed to a directional light source, adult zebrafish display a positive phototactic response (Movies S1 and S2) [32]. We hypothesized that TH-treated wild-type fish would have a stronger phototactic response to near-infrared light than *cyp27c1D1/D3* mutants due to the vitamin A2-induced red-shift in spectral sensitivity.

We compared the behavior of dark-adapted, vehicle- and TH-treated *cyp27c1D1/D3* and wild-type siblings in response to 590-nm and 770-nm light (Figure 5; see Figure S4 for LED characterization). Fish with vitamin A1- and A2-based photopigments are predicted to perceive 590-nm light similarly, based on the sensitivity curves of red cones (Figure 5B). As expected, in both the vehicle and TH treatments, *cyp27c1D1/D3* mutants and wild-type fish exhibited positive phototaxis toward a 590-nm light source (Figure 5D). This finding indicates that normal visually mediated behaviors are intact and functional in *cyp27c1D1/D3* mutants. In contrast, upon exposure to 770-nm light, only wild-type, TH-treated fish demonstrated a positive phototactic response, whereas *cyp27c1D1/D3* mutants and vehicle control fish behaved as if they were in the dark (Figure 5E). These data indicate that the red-shift in photoreceptor spectral sensitivity caused by switching to vitamin A2-based photopigments improves the animal's ability to detect and respond to near-infrared light. This increase in long-wavelength sensitivity may provide a selective advantage under some environmental conditions and may thus have contributed to the evolution of the rhodopsin-porphyrin system.

### **DISCUSSION**

We have shown that the action of a single enzyme, *Cyp27c1*, is necessary and sufficient for the production of vitamin A2 and its derivatives and for the resultant red-shift in photoreceptor spectral sensitivity. Furthermore, we have demonstrated that this change in sensitivity at the cellular level can be translated into altered behavioral responsiveness to long-wavelength light. These findings assign a biochemical function to a previously orphan member of the cytochrome P450 family of enzymes. In addition, the generation of *cyp27c1* mutants offers an opportunity to study the behavioral consequences of switching from vitamin A1- to vitamin A2-based photopigments.



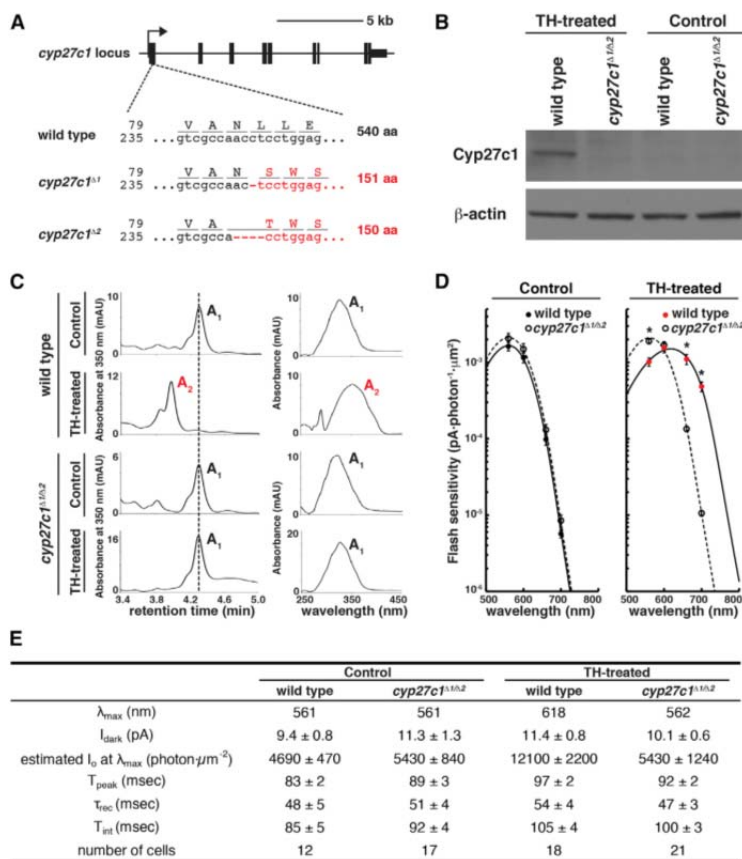


**Figure 4. Cyp27c1 Is Necessary for Vitamin A<sub>2</sub> Production and Red-Shifting of Photoreceptors In Vivo**

(A) TALENs were used to generate *cyp27c1* mutant zebrafish. Two independent alleles are shown, *cyp27c1*<sup>D1</sup> and *cyp27c1*<sup>D2</sup>. Both alleles contain frame-shift mutations resulting in premature stop codons at amino acids 151 and 150, respectively. (B) Western blot with rabbit polyclonal anti-Cyp27c1 antibody shows that Cyp27c1 protein is detected in the RPE of wild-type fish, but not in the RPE of *cyp27c1*<sup>D1/D2</sup> fish, after 3 weeks of TH treatment.  $\beta$ -actin was used as a loading control. (C) Wild-type and *cyp27c1*<sup>D1/D2</sup> siblings were treated with TH or vehicle control for 3 weeks, and retinas and RPE from three animals were pooled and analyzed for retinoid content using HPLC. A TH-driven switch to vitamin A<sub>2</sub> was observed in wild-type fish, but not in *cyp27c1*<sup>D1/D2</sup> mutants. (D) The spectral sensitivity of red cones from TH-treated *cyp27c1*<sup>D1/D2</sup> fish and their wild-type siblings was assessed using single-cell suction electrode recording. The photoreceptors were exposed to a series of dim flashes at 560, 600, 660, and 700 nm, and their response amplitudes were used to calculate flash sensitivity (y axis) as a function of wavelength (x axis). No significant difference was observed between vehicle-treated *cyp27c1*<sup>D1/D2</sup> and wild-type red cones. However, TH-treated wild-type red cones were significantly more sensitive to 660- and 700-nm light and less sensitive to 560-nm light relative to *cyp27c1*<sup>D1/D2</sup> red cones (Student's t test; \* $p < 0.0005$ ;  $n = 12-21$ ; error bars = SEM). Fitted curves were calculated using a model that incorporates both vitamin A<sub>1</sub>- and A<sub>2</sub>-based pigment. This model predicts 100% vitamin A<sub>1</sub> in vehicle-treated wild-type and *cyp27c1*<sup>D1/D2</sup> fish, 99.7% vitamin A<sub>1</sub> in TH-treated *cyp27c1*<sup>D1/D2</sup> fish, and 95.5% vitamin A<sub>2</sub> in TH-treated wild-type siblings. (E) Physiological parameters of the red cones are indicated  $\pm$  SEM. These include wavelength of peak sensitivity ( $I_{max}$ ), dark current ( $I_{dark}$ ), estimated half-saturation light intensity at  $I_{max}$  ( $I_{0.5}$ ), dimflash response time to peak ( $T_{peak}$ ), recovery time constant ( $\tau_{rec}$ ; estimated from a single-exponential fit to the tail of the response), and integration time ( $T_{int}$ ; estimated as the time integral of the normalized flash response). See also Figure S3.

Our work raises a number of intriguing questions about the role of Cyp27c1 in vivo. For example, the preferred substrate(s) of Cyp27c1 in vivo is currently unknown. A number of potential substrates are present in the RPE, including all-trans retinol, all-trans retinyl esters, 11-cis retinol, 11-cis retinal, or even 11-cis retinyl esters [20, 33]. Our cell-free assays suggest that all-trans retinol could be the in vivo substrate, but future studies will be needed to measure the activity of Cyp27c1 on 11-cis retinoids and characterize the retinoids metabolized by Cyp27c1 in vivo. Interestingly, whereas some enzymes involved in the visual cycle (LRAT, RPE65, and 11cRDH) are localized to the smooth ER, prediction algorithms suggest that Cyp27c1 may be located in mitochondria, as are Cyp27a1 and Cyp27b1 [20, 34, 35]. The subcellular localization of Cyp27c1 and the pathways by which retinoids might be trafficked between cellular organelles also remain open questions.

The ability of TH to induce the expression of *cyp27c1* raises the possibility that endogenous TH might play a general role in the regulation of responsiveness to long-wavelength light under natural conditions. For instance, TH is thought to play a key role in coordinating the physiologic changes that salmonids undergo during migration, suggesting that TH may mediate the switch between vitamin A<sub>1</sub>- and A<sub>2</sub>-based photopigments in these animals [36, 37]. In addition, the salmon genome contains multiple paralogous red and green cone opsin genes and TH treatment induces a shift in the expression of these opsins in favor of the red-shifted paralogs [37]. Lastly, both zebrafish and mice require thyroid hormone receptor b2 for normal expression of long wavelength-sensitive

cone opsin [38, 39]. These findings suggest that TH signaling might represent an ancient pathway for the regulation of sensitivity to long-wavelength light, both at the level of chromophore modification and opsin gene expression.

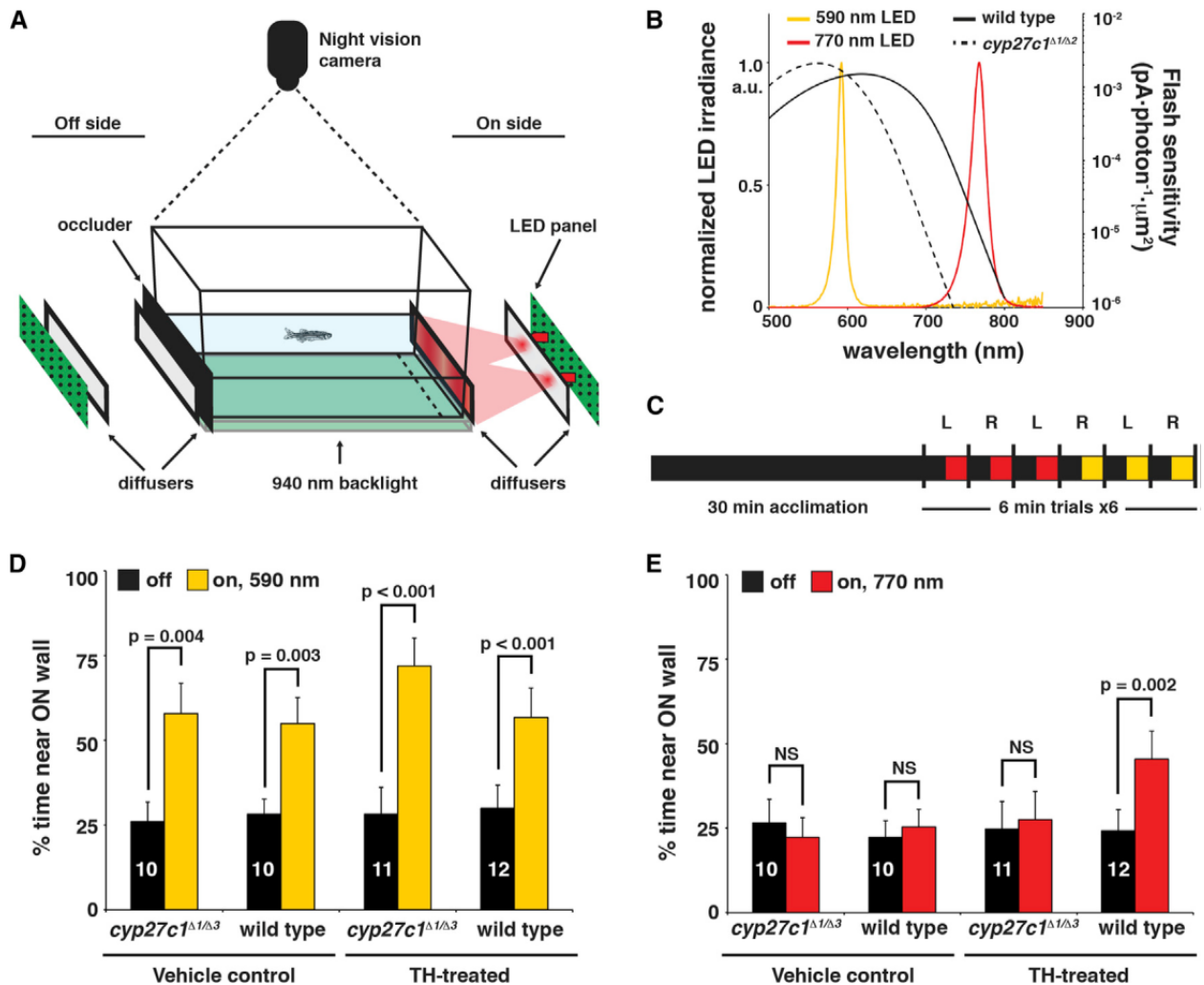


**Figure 5. Mutation of Cyp27c1 Abolishes the Phototactic Response to Near-Infrared Light**

(A) The phototaxis assay consisted of 590- or 770-nm LED light sources placed on either the right or left side of a tank (depicted on the right side in the schematic). Light from the LEDs passed through two diffusers before illuminating one end of the tank. On the opposite end of the tank, a black occluder was inserted to prevent reflection off of the "off-side" diffuser. Fish movement was recorded using a night vision camera and a 940-nm infrared backlight located beneath the tank. The percentage of time spent within 25 mm of the lit "on" side (dashed line) was determined. The behavioral assay and subsequent data analysis were conducted in a blinded fashion with respect to the genotype of the fish.

(B) A comparison of red cone sensitivity data (reproduced from Figure 4D) and the measured LED spectra.

(C) Summary of the experimental design. Each dark-adapted fish was acclimated to the testing tank for 30 min in the dark and then recorded during a set of three trials each at 770 and 590 nm. Each trial consisted of 3 min dark and 3 min lit conditions, with the order of light/dark presentation randomized. The light source was alternated between the left and right sides for each trial.

(D) TH- and vehicle-treated *cyp27c1 $\Delta$ 1/3* mutants and wild-type siblings all showed a significant positive phototactic response to 590-nm light (paired Student's t test;  $p < 0.005$ ; n as indicated per group; error bars = SEM). All p values remained significant after Bonferroni correction for multiple testing.

(E) Only TH-treated wild-type fish showed a significant positive phototactic response to 770-nm light. For significantly different groups, p values are as shown. For vehicle-treated *cyp27c1 $\Delta$ 1/3* mutant and wild-type fish at 770 nm, p values were 0.449 and 0.177, respectively. For TH-treated *cyp27c1 $\Delta$ 1/3* mutants at 770 nm, the p value was 0.490 (paired t test; n as indicated per group; error bars = SEM). All p values remained significant after Bonferroni correction for multiple testing.

See also Figure S4 and Movies S1 and S2.

Despite the widespread use of the rhodopsin-porphyrin system among cold-blooded vertebrates, vitamin A2-based photopigments have never been documented in the eyes of birds or mammals. One possible explanation for this absence is that A2-based chromophores are less thermally stable than those based on A1. Thus, increased thermal noise may limit the usefulness of A2 chromophores in the visual systems of warm-blooded species. Nevertheless, orthologs of *cyp27c1* are present in nearly all sequenced avian genomes as well as most mammalian genomes,

including the human genome. The function of *cyp27c1* in these species is currently unknown, but several studies suggest diverse roles for this gene outside of the eye. For example, 3,4-didehydroretinoic acid (a derivative of vitamin A2) has been reported to have biological activity similar to retinoic acid in chicken embryos and is the predominant form of “retinoic acid” in the developing chick [40, 41]. In addition, the presence of 3,4-didehydroretinoids has been documented in normal human skin (and at elevated levels in hyperkeratotic lesions and some skin neoplasms), suggesting a potential role for CYP27C1 in retinoid biosynthesis in this organ [42, 43]. Future studies will be needed to address the role of *cyp27c1* in these contexts.

Further work may explore the extent of *Cyp27c1* expression and function in the visual systems of different species. A recent study demonstrated that the ratio of vitamin A1 to A2 can vary between rods and cones in the same retina [44]. This finding raises the possibility that *Cyp27c1* might be differentially expressed between these two cell types in some species. Alternatively, these species might express *Cyp27c1* in Müller glia, a cell type that supports cone, but not rod, pigment regeneration [21]. It is also worth noting that vitamin A2-based chromophores are known to be used in some invertebrate species. This fact suggests that functional homologs of *Cyp27c1* could be widespread in the animal kingdom.

The present study also has important implications for the field of optogenetics. Optogenetic actuators are microbial opsins that use retinal as a chromophore and can modulate the electrical activity of neurons in response to light [45]. Actuators with redshifted excitation spectra are highly desirable, because longerwavelength light penetrates more deeply into tissue and redshifting reduces spectral overlap with co-expressed sensors. Accordingly, several research groups have created red-shifted optogenetic actuators either by bioprospecting for novel actuators with red-shifted excitation spectra or by generating redshifted variants of known actuators by protein engineering [46–49]. It was recently shown that the sensitivity of optogenetic actuators can be red-shifted *in vitro* when the chromophore, 3,4-didehydroretinal, is substituted for retinal [50]. This finding suggests that co-expression of *Cyp27c1* could be used to red-shift optogenetic actuators into the near infrared in selected neuronal populations *in vivo*.

## EXPERIMENTAL PROCEDURES

See the Supplemental Experimental Procedures for detailed experimental procedures.

### Animals and Thyroid Hormone Treatment

All procedures were carried out in accordance with animal protocols approved by the Animal Studies Committee of Washington University. Adult zebrafish (>3 months old) were used for all experiments. The specific strains include WT AB\* and SJD, albino, *cyp27c1D1*, *cyp27c1D2*, *cyp27c1D3*, *cyp27c1D4*, and *cyp27c1D5*. The *cyp27c1* transgenic lines were generated using TALENs targeting exon 1 (D1–D4) and exon 4 (D5). This strategy generated short indels that resulted in frameshift mutations leading to premature stop codons. TH treatment consisted of a 3-week incubation in either TH (750 ml 400 mg/ml L-thyroxine in 0.1 M NaOH per liter of water for a final concentration of 300 mg/l) or vehicle control (750 ml of 0.1 M NaOH per liter of water). Bullfrog eyes were obtained post-mortem.

### HPLC

Conditions for HPLC were selected to isolate retinal and retinol. Tissue from zebrafish and bullfrog was isolated, frozen on dry ice, and stored at 80°C prior to use. Retinoids were extracted in hexanes and dried under nitrogen. Retinal was then converted to retinol

by treating the sample with NaBH<sub>4</sub> prior to drying under nitrogen and resuspension in acetonitrile. Reverse-phase HPLC was conducted on an Agilent 1100 Series HPLC system equipped with a YMC carotenoid 5.0 mm column (4.6 mm  $\times$  250 mm; cat no. 924012; YMC America). For the tissue samples, we injected 90  $\mu$ l of sample and eluted isocratically with a mobile phase of acetonitrile:methanol:dichloromethane 70:15:15 (vol:vol:vol) at a flow rate of 1 ml min<sup>-1</sup> and a column temperature of 18°C.

HPLC was also conducted on HEK293 cells, which had been transfected with Cyp27c1 or an empty vector and supplied with vitamin A1 as a substrate (further described in the Supplemental Experimental Procedures). Retinoids were extracted from the HEK293 cells and their media as above and resuspended in mobile phase. These samples were eluted isocratically with a mobile phase of acetonitrile:water 80:20 (vol:vol) at a flow rate of 1 ml min<sup>-1</sup> and column temperature of 18°C. Retinol (vitamin A1) and 3,4-didehydroretinol (vitamin A2) were identified by comparison with authentic standards obtained from Sigma (R7632) and Santa Cruz Biotechnology (sc-209587), respectively.

### **RNA-Seq and qRT-PCR**

RNA was isolated from zebrafish and bullfrog RPE using an RNeasy kit. Zebrafish cDNA libraries were generated using NuGen Ovation RNA-Seq System v2, whereas bullfrog mRNA was enriched using the Illumina Ribo-Zero kit. Samples were assayed for quality and quantity and sequenced on an Illumina HiSeq 2500 using single-end 50-bp reads. The reads were aligned and differential expression analysis was conducted as described in the Supplemental Experimental Procedures. qRT-PCR was conducted on the same samples used for RNA-seq to confirm these results. Primer sequences and other details related to qRT-PCR are listed in the Supplemental Experimental Procedures.

### **In Situ Hybridization, Immunohistochemistry, and Western Blotting**

For in situ hybridization (ISH) and immunohistochemistry, 12-mm frozen sections were collected at or adjacent to the level of the optic nerve head. The approach and probes used for ISH are described in the Supplemental Experimental Procedures. To generate an antibody for IHC and western blot, we created a peptide fragment encompassing amino acids 293–482 of zebrafish Cyp27c1, which was used by PrimmBiotech to immunize two rabbits and three rats PrimmBiotech. This antibody was used for IHC and western blotting as described in the Supplemental Experimental Procedures.

### **Enzyme Kinetic Assays**

The reaction mixtures contained recombinant zebrafish Cyp27c1, bovine adrenodoxin (Adx), bovine NADPH-adrenodoxin reductase (ADR), potassium phosphate (50 mM), and various concentrations of a retinoid substrate, which were added to an amber vial and pre-incubated in a water bath at 37°C prior to initiation with an NADPH-generating system. Following a 60 s incubation, the reaction was quenched with 1.0 ml of ethyl acetate solution containing 45 mM butylated hydroxytoluene (to prevent radical reactions). The organic solvent was extracted, dried under nitrogen, and resuspended in CH<sub>3</sub>CN (100  $\mu$ l). HPLC-UV was used to separate and detect the products. Briefly, 10  $\mu$ l of the sample was injected onto a Hypersil GOLD HPLC column (150 mm  $\times$  2.1 mm; 3 mm; Thermo Scientific) at 40°C and the products were eluted isocratically (0.5 ml/min) at 30% solvent A (95% H<sub>2</sub>O; 4.9% CH<sub>3</sub>CN; 0.1% formic acid, v/v) and 70% solvent B (95% CH<sub>3</sub>CN; 4.9% H<sub>2</sub>O; 0.1% formic acid, v/v) at a flow rate of 0.5 ml/min. Data

analysis and graph generation were conducted using GraphPad Prism v. 5.0d, using a single-site hyperbolic equation.

### **Single-Cell Suction Electrode Recording**

Cell preparation was carried out under dim red light. Photoreceptors were dissociated by chopping and triturating the retina in Ringer solution and transferred to the recording chamber, where they were perfused with Ringer solution. Red cones were identified based on their characteristic morphology and relatively high photosensitivity at 700 nm. Under infrared illumination, the inner segment of a red cone was drawn into a tight-fitting glass pipette for recordings and stimulated with calibrated 20 ms flashes centered at 560, 600, 660, and 700 nm. The light source was calibrated before and after each experiment. The signals were low-pass filtered at 30 Hz (8-pole Bessel), digitized at 1 kHz, and stored on a computer using Clampex 9.2 acquisition software (Molecular Devices). Data were analyzed using Clampfit (Molecular Devices) and Origin 8.1 (OriginLab).

### **Phototaxis Assay**

The recording setup consisted of a clear plastic rectangular tank (19 cm 3 35 cm) with a diffuse light source located across either the right or left end of the tank. The light source was equipped with a switch to toggle between 590 and 770-nm LEDs and a variable resistor to control illuminance. The fish were recorded with Sony HDR-SR11 video camera using a 940-nm backlight. The behavioral trials were conducted in a dark interior room with no windows. The immediate recording area (tank, light sources, and camera) was draped with a double layer of black fleece and monitored periodically using a small monitor covered in red plastic located outside of the draping.

We assayed 11 TH-treated *cyp27c1D1/D3* mutants, 12 TH-treated wildtypes, ten vehicle-treated *cyp27c1D1/D3* mutants, and ten TH-treated wildtype. One TH-treated *cyp27c1D1/D3* mutant was excluded, as it exhibited erratic swimming behavior. Fish were dark adapted overnight and transferred individually to the recording tank. After acclimating in the dark for 30 min, each fish was recorded for three trials at 770 nm and then three trials at 590 nm. Each trial consisted of 3 min with the LEDs on and 3 min with the LEDs off, with the on/off order randomized. We also alternated the end of the tank illuminated in each trial. We tracked the paths of individual fish using an image difference approach with code written in Matlab (Release 2104a; The Math- Works). We then calculated the percentage of time spent within 25 mm of the lit wall of the tank. The difference in mean time (as a percentage) spent against the lit end when LED lights were on and off was compared within groups with paired Student's *t* tests (SPSS, version 21; IBM).

### **ACCESSION NUMBERS**

The accession number for the raw sequence files, the fasta files used for alignment, and the full output of edgeR for zebrafish and bullfrog reported in this paper is GEO: GSE69219.

### **SUPPLEMENTAL INFORMATION**

Supplemental Information includes five figures, two tables, Supplemental Experimental Procedures, and two movies and can be found with this article online at

<http://dx.doi.org/10.1016/j.cub.2015.10.018>.

### **AUTHOR CONTRIBUTIONS**

J.M.E. and J.C.C. conceived and coordinated the study. J.M.E. conducted expression profiling, genetic analysis, in situ hybridization and antibody staining, western blotting, generation and maintenance

of transgenic lines, and behavioral assays. J.R.A. and S.L.J. were involved in initial TH treatment experiments and enzyme assays. S.E.T. consulted on the design of the behavioral assay and conducted analysis of behavioral data. M.J.H. and N.W.R. provided software for analysis of behavioral data as well as other support. M.B.T. produced the anti-Cyp27c1 antibody. J.M.E. and M.B.T. performed retinoid analyses. S.S. and V.J.K. performed single-cell suction electrode recordings and analyzed the resultant data. R.F., V.M.K., L.D.N., K.M.J., Y.X., and F.P.G. conducted in vitro biochemical assays and analyzed the resultant data. J.M.E. and J.C.C. wrote and all authors edited and approved the manuscript.

## ACKNOWLEDGMENTS

We dedicate this paper to the memory of Dr. David Beebe. We thank S. Shen, C. Micchelli, J. Gusdorf, P. Connelly, S. Miller, S. Canter, E. Sanders, and J. Engelhard for advice and technical assistance. We thank P. Widder for supplying bullfrog tissue. This work was supported by grants from the Human Frontier Science Program (to J.C.C. and N.W.R.); from the NIH, EY024958 (to J.C.C.), 8 *Current Biology* 25, 1–10, December 7, 2015 ©2015 Elsevier Ltd All rights reserved Please cite this article in press as: Enright et al., Cyp27c1 Red-Shifts the Spectral Sensitivity of Photoreceptors by Converting Vitamin A1 into A2, *Current Biology* (2015), <http://dx.doi.org/10.1016/j.cub.2015.10.018> EY019312 (to V.J.K.), GM056988 (to S.L.J.), CA090426 (to F.P.G.), F31 NS083170 (to J.M.E.), T32 EY013360 (to J.M.E.), T32 ES007028 (to V.M.K.), and T32 CA009582 (to K.M.J.); from Research to Prevent Blindness (to J.C.C. and V.J.K.); and from the Air Force Office of Scientific Research (FA8655-12-2112 to N.W.R.). We acknowledge the support of the Genome Technology Access Center at Washington University (P30 CA91842 and UL1 TR000448; NIH) and the Vision Core Electronics Services Module (P30 EY002687; NIH).

Received: September 4, 2015

Revised: October 4, 2015

Accepted: October 6, 2015

Published: November 5, 2015

## REFERENCES

1. Wald, G. (1968). Molecular basis of visual excitation. *Science* 162,230–239.
2. Burns, M.E., and Baylor, D.A. (2001). Activation, deactivation, and adaptation in vertebrate photoreceptor cells. *Annu. Rev. Neurosci.* 24, 779–805.
3. Yokoyama, S. (2000). Molecular evolution of vertebrate visual pigments. *Prog. Retin. Eye Res.* 19, 385–419.
4. Wang, W., Geiger, J.H., and Borhan, B. (2014). The photochemical determinants of color vision: Revealing how opsins tune their chromophore's absorption wavelength. *BioEssays* 36, 65–74.
5. Goldsmith, T.H. (1990). Optimization, constraint, and history in the evolution of eyes. *Q. Rev. Biol.* 65, 281–322.
6. Köttgen, E., and Abelsdorff, G. (1896). Absorption and Zersetzung des Sehpurpurs bei den Wirbeltieren. *Z. Psychol. Physiol. Sinnesorg.* 12, 161–184.
7. Kühne, W., and Sewall, H. (1880). Zur Physiologie des Sehepithels, insbesondere der Fische. *Untersuch. Physiol. Inst. Univ. Heidelberg* 3, 221. 8. Govardovskii, V.I., Fyhrquist, N., Reuter, T., Kuzmin, D.G., and Donner, K. (2000). In search of the visual pigment template. *Vis. Neurosci.* 17, 509–528.
9. Beatty, D.D. (1966). A study of the succession of visual pigments in Pacific salmon (*Oncorhynchus*). *Can. J. Zool.* 44, 429–455.
10. Liebman, P.A., and Entine, G. (1968). Visual pigments of frog and tadpole (*Rana pipiens*). *Vision Res.* 8, 761–775.
11. Wald, G. (1957). The metamorphosis of visual systems in the sea lamprey. *J. Gen. Physiol.* 40, 901–914. 12. Reuter, T.E., White, R.H., and Wald, G.

- (1971). Rhodopsin and porphyropsin fields in the adult bullfrog retina. *J. Gen. Physiol.* 58, 351–371.
13. Surface, H.A. (1913). First report on the economic features of the amphibians of Pennsylvania. *Zool. Bull. Div. Zool. Pa. Dept. Agric.* 3, 65.
  14. Wald, G. (1939). The porphyropsin visual system. *J. Gen. Physiol.* 22, 775–794.
  15. Bridges, C.D.B. (1972). The rhodopsin-porphyrpsin visual system. In *Handbook of Sensory Physiology VII/1*, H.H.A. Dartnall, ed. (Springer-Verlag), pp. 417–480.
  16. Toyama, M., Hironaka, M., Yamahama, Y., Horiguchi, H., Tsukada, O., Uto, N., Ueno, Y., Tokunaga, F., Seno, K., and Hariyama, T. (2008). Presence of rhodopsin and porphyropsin in the eyes of 164 fishes, representing marine, diadromous, coastal and freshwater species—a qualitative and comparative study. *Photochem. Photobiol.* 84, 996–1002.
  17. Wilt, F.H. (1959). The differentiation of visual pigments in metamorphosing larvae of *Rana catesbeiana*. *Dev. Biol.* 1, 199–233.
  18. Temple, S.E., Plate, E.M., Ramsden, S., Haimberger, T.J., Roth, W.M., and Hawryshyn, C.W. (2006). Seasonal cycle in vitamin A1/A2-based visual pigment composition during the life history of coho salmon (*Oncorhynchus kisutch*). *J. Comp. Physiol. A Neuroethol. Sens. Neural Behav. Physiol.* 192, 301–313.
  19. Allison, W.T., Haimberger, T.J., Hawryshyn, C.W., and Temple, S.E. (2004). Visual pigment composition in zebrafish: Evidence for a rhodopsin-porphyrpsin interchange system. *Vis. Neurosci.* 21, 945–952.
  20. Saari, J.C. (2012). Vitamin A metabolism in rod and cone visual cycles. *Annu. Rev. Nutr.* 32, 125–145.
  21. Wang, J.S., and Kefalov, V.J. (2011). The cone-specific visual cycle. *Prog. Retin. Eye Res.* 30, 115–128.
  22. Coon, M.J. (2005). Cytochrome P450: nature’s most versatile biological catalyst. *Annu. Rev. Pharmacol. Toxicol.* 45, 1–25.
  23. Guengerich, F.P., and Cheng, Q. (2011). Orphans in the human cytochrome P450 superfamily: approaches to discovering functions and relevance in pharmacology. *Pharmacol. Rev.* 63, 684–699.
  24. Nelson, D.R., Koymans, L., Kamataki, T., Stegeman, J.J., Feyereisen, R., Waxman, D.J., Waterman, M.R., Gotoh, O., Coon, M.J., Estabrook, R.W., et al. (1996). P450 superfamily: update on new sequences, gene mapping, accession numbers and nomenclature. *Pharmacogenetics* 6, 1–42.
  25. Wu, Z.L., Bartleson, C.J., Ham, A.J., and Guengerich, F.P. (2006). Heterologous expression, purification, and properties of human cytochrome P450 27C1. *Arch. Biochem. Biophys.* 445, 138–146.
  26. Tsetskhladze, Z.R., Canfield, V.A., Ang, K.C., Wentzel, S.M., Reid, K.P., Berg, A.S., Johnson, S.L., Kawakami, K., and Cheng, K.C. (2012). Functional assessment of human coding mutations affecting skin pigmentation using zebrafish. *PLoS ONE* 7, e47398.
  27. Lutz, J.D., Dixit, V., Yeung, C.K., Dickmann, L.J., Zelter, A., Thatcher, J.E., Nelson, W.L., and Isoherranen, N. (2009). Expression and functional characterization of cytochrome P450 26A1, a retinoic acid hydroxylase. *Biochem. Pharmacol.* 77, 258–268.
  28. Nakayama, K., Puchkaev, A., and Pikuleva, I.A. (2001). Membrane binding and substrate access merge in cytochrome P450 7A1, a key enzyme in degradation of cholesterol. *J. Biol. Chem.* 276, 31459–31465.
  29. Pallan, P.S., Wang, C., Lei, L., Yoshimoto, F.K., Auchus, R.J., Waterman, M.R., Guengerich, F.P., and Egli, M. (2015). Human cytochrome P450 21A2, the major steroid 21-hydroxylase: structure of the enzyme-progesterone substrate complex and rate-limiting C-H bond cleavage. *J. Biol. Chem.* 290, 13128–13143.
  30. Shinkyo, R., and Guengerich, F.P. (2011). Cytochrome P450 7A1 cholesterol 7 $\alpha$ -hydroxylation: individual reaction steps in the catalytic cycle and rate-limiting ferric iron reduction. *J. Biol. Chem.* 286, 4632–4643.
  31. Dahlem, T.J., Hoshijima, K., Jurynek, M.J., Gunther, D., Starker, C.G., Locke, A.S., Weis, A.M., Voytas, D.F., and Grunwald, D.J. (2012). Simple methods for generating and detecting locus-specific mutations induced with TALENs in the zebrafish genome. *PLoS Genet.* 8, e1002861.
  32. Shcherbakov, D., Kno“rzer, A., Espenhahn, S., Hilbig, R., Haas, U., and Blum, M. (2013). Sensitivity differences in fish offer near-infrared vision as an adaptable evolutionary trait. *PLoS ONE* 8, e64429.
  33. Babino, D., Perkins, B.D., Kindermann, A., Oberhauser, V., and von Lintig, J. (2015). The role of 11-cis-retinyl esters in vertebrate cone vision. *FASEB J.* 29, 216–226.
  34. Saarem, K., Bergseth, S., Oftebro, H., and Pedersen, J.I. (1984). Subcellular localization of vitamin D3 25-hydroxylase in human liver. *J. Biol. Chem.* 259, 10936–10940.
  35. Saarem, K., Pedersen, J.I., and Tollersrud, S. (1978). Soluble 25-hydroxyvitamin D3-1  $\alpha$ -hydroxylase from kidney mitochondria of rachitic pigs. *Comp. Biochem. Physiol. B* 61, 485–490.
  36. Beatty, D.D. (1969). Visual pigment changes in juvenile kokanee salmon in response to thyroid hormones. *Vision Res.* 9, 855–864.
  37. Temple, S.E., Ramsden, S.D., Haimberger, T.J., Veldhoen, K.M., Veldhoen, N.J., Carter, N.L., Roth, W.M., and Hawryshyn, C.W. (2008). Effects of



- exogenous thyroid hormones on visual pigment composition in coho salmon (*Oncorhynchus kisutch*). *J. Exp. Biol.* 211, 2134–2143.
38. Ng, L., Hurley, J.B., Dierks, B., Srinivas, M., Salto´, C., Vennstro¨m, B., Reh, T.A., and Forrest, D. (2001). A thyroid hormone receptor that is required for the development of green cone photoreceptors. *Nat. Genet.* 27, 94–98.
39. Suzuki, S.C., Bleckert, A., Williams, P.R., Takechi, M., Kawamura, S., and Wong, R.O. (2013). Cone photoreceptor types in zebrafish are generated by symmetric terminal divisions of dedicated precursors. *Proc. Natl. Acad. Sci. USA* 110, 15109–15114.
40. Maden, M., Sonneveld, E., van der Saag, P.T., and Gale, E. (1998). The distribution of endogenous retinoic acid in the chick embryo: implications for developmental mechanisms. *Development* 125, 4133–4144.
41. Thaller, C., and Eichele, G. (1990). Isolation of 3,4-didehydroretinoic acid, a novel morphogenetic signal in the chick wing bud. *Nature* 345, 815–819.
42. Rollman, O., and Vahlquist, A. (1985). Vitamin A in skin and serum—studies of acne vulgaris, atopic dermatitis, ichthyosis vulgaris and lichen planus. *Br. J. Dermatol.* 113, 405–413.
43. Vahlquist, A. (1980). The identification of dehydroretinol (vitamin A2) in human skin. *Experientia* 36, 317–318.
44. Saarinen, P., Pahlberg, J., Herczeg, G., Viljanen, M., Karjalainen, M., Shikano, T., Merila¨, J., and Donner, K. (2012). Spectral tuning by selective chromophore uptake in rods and cones of eight populations of nine-spined stickleback (*Pungitius pungitius*). *J. Exp. Biol.* 215, 2760–2773.
45. Zhang, F., Vierock, J., Yizhar, O., Fenno, L.E., Tsunoda, S., Kianianmomeni, A., Prigge, M., Berndt, A., Cushman, J., Polle, J., et al. (2011). The microbial opsin family of optogenetic tools. *Cell* 147, 1446–1457.
46. Chuong, A.S., Miri, M.L., Busskamp, V., Matthews, G.A., Acker, L.C., Sørensen, A.T., Young, A., Klapoetke, N.C., Henninger, M.A., Kodandaramaiah, S.B., et al. (2014). Noninvasive optical inhibition with a red-shifted microbial rhodopsin. *Nat. Neurosci.* 17, 1123–1129.
47. Govorunova, E.G., Spudich, E.N., Lane, C.E., Sineshchekov, O.A., and Spudich, J.L. (2011). New channelrhodopsin with a red-shifted spectrum and rapid kinetics from *Mesostigma viride*. *MBio* 2, e00115-11.
48. Lin, J.Y., Knutsen, P.M., Muller, A., Kleinfeld, D., and Tsien, R.Y. (2013). ReaChR: a red-shifted variant of channelrhodopsin enables deep transcranial optogenetic excitation. *Nat. Neurosci.* 16, 1499–1508.
49. Zhang, F., Prigge, M., Beyrie`re, F., Tsunoda, S.P., Mattis, J., Yizhar, O., Hegemann, P., and Deisseroth, K. (2008). Red-shifted optogenetic excitation: a tool for fast neural control derived from *Volvox carteri*. *Nat. Neurosci.* 11, 631–633.
50. Sineshchekov, O.A., Govorunova, E.G., Wang, J., and Spudich, J.L. (2012). Enhancement of the long-wavelength sensitivity of optogenetic microbial rhodopsins by 3,4-dehydroretinal. *Biochemistry* 51, 4499–4506.